Pflugers Arch - Eur J Physiol (2012) 463:585–592
DOI 10.1007/s00424-012-1077-z

ION CHANNELS, RECEPTORS AND TRANSPORTERS

Pannexin 1 forms an anion-selective channel

Weihong Ma · Vincent Compan · Wenxuan Zheng · Elizabeth Martin · R. Alan North · Alexei Verkhratsky · Annmarie Surprenant

Received: 8 January 2012 / Accepted: 24 January 2012 / Published online: 7 February 2012

Abstract Pannexin 1 (Panx1) is expressed in various mammalian tissues including the brain and immune cells. Here, we present evidence that Panx1 when expressed in mammalian cells, forms anion-selective channels, with a rank order of permeabilities: $NO_3^- > I^- > Br^- > Cl^- > F^- \gg$ aspartate$^-$ ≈ glutamate$^-$ ≈ gluconate$^-$. Single-channel Panx1-mediated currents have a unitary conductance around 68 pS. Our results show that Panx1 assembles into a membrane anion channel with a relatively low single-channel conductance.

Keywords Pannexin 1 · HEK293 · Anion channel · Single channel

Introduction

Pannexin 1 (Panx1) is the most ubiquitous of the three members of the pannexin gene family [20, 21]. Protein and mRNA have been detected in a range of mammalian tissues, including the brain and immune cells [4, 20, 23]. The amino acid sequence has low homology with gap junction-forming invertebrate proteins innexins [2]. Accordingly, pannexins have been considered to be similar to vertebrate gap junction-forming channels connexins (Cx), with a hexameric structure [26] and the ability to form large transmembrane pores [1, 4, 15].

Further studies however demonstrated that Panx1 sequences are not closely related to those of connexins [2, 20] and, with the exception of a study on manually paired oocytes [4], there is little evidence that pannexins form gap junctions [10, 22]. Furthermore, in contrast to connexins, Panx1 currents are not sensitive to inhibition by extracellular divalent cations [4]. It has been suggested that Panx1 channels can be regulated by cytosolic Ca^{2+} [15]; however, this has not been confirmed in subsequent experiments [16]. Panx1 has also been proposed to serve as a conduit for release of ATP from erythrocytes, taste bud cells, airway epithelia and possibly in CA3 hippocampal neurones [11, 13, 15, 24]. The Panx1 channel opening is typically triggered by depolarisation in over-expression systems [5, 16], although channel activation has been also detected in response to mechanical stimulation in oocyte expression system and possibly in erythrocytes [1, 14] (but see [25]), to osmotic stress in airway epithelial cells [24], or following *N*-methyl-D-aspartate receptor activation in hippocampal neurones [28].

Our previous studies made in Panx1-overexpressing human embryonic kidney (HEK) 293 cells confirmed main electrophysiological properties of Panx1-mediated currents as obtained in oocytes. We found that the outwardly rectifying Panx1 currents are activated at voltages more positive than ~10 mV, that these currents are more sensitive to carbenoxolone (CBX) when compared to Cx-mediated currents, and that Panx1 currents are insensitive to extracellular calcium [16]. In this paper, we present a more detailed characterisation of the biophysical

Weihong Ma and Vincent Compan contributed equally to the study.

W. Ma · V. Compan · W. Zheng · E. Martin · R. A. North · A. Verkhratsky (✉) · A. Surprenant
Faculty of Life Sciences, The University of Manchester,
Smith Building, Oxford Road,
Manchester M13 9PT, UK
e-mail: Alexej.Verkhratsky@manchester.ac.uk

Present Address:
W. Ma
Manchester Medical School,
Faculty of Medical and Human Sciences,
The University of Manchester,
Oxford Road,
Manchester M13 9PT, UK

properties of Panx1 channel expressed in HEK293 cells. We found that Panx1 is permeable to chloride and other anions. In addition, Panx1 exhibits a relatively low single-channel conductance compared with connexins.

Experimental details

Materials

All the salts and drugs were purchased from Sigma–Aldrich (Poole, UK) unless otherwise stated. 4-[(2-Butyl-6,7-dichloro-2-cyclopentyl-2,3-dihydro-1-oxo-1H inden-5-yl) oxy]butanoic acid (DCPIB) was from Tocris (Bristol, UK). Sulfo-NHS-LC-biotin and streptavidin–horseradish peroxidase (HRP) were purchased from Pierce (Cramlington, UK). The Myc antibody was from Covance (Harrogate, UK). Streptavidin–Texas Red was from Vector laboratories (Peterborough, UK). Cell culture media (DMEM:F12 and Optimem) and lipofectamine were supplied by Invitrogen.

Cell culture and transfection

HEK 293 cells (American Type Culture Collection, ATCC, Teddington, UK, ATCC no. CRL-1573) were maintained in DMEM/F12 (1:1) medium supplemented with 10% foetal calf serum (FCS) and 2 mM glutamine (Invitrogen). Lipofectamine 2000 reagent (Invitrogen) was used for transfecting HEK cells under manufacturer's instructions. Briefly, 1 μg (unless otherwise stated) of plasmid DNA and 0.1 μg of a plasmid encoding e-GFP (where necessary) were mixed with 3 μl of lipofectamine in Optimem. The mixture was transferred to a 35-mm petri dish of HEK cells. Cells were normally incubated in the DNA-lipofectamine medium for 4 to 24 h before being plated on to coverslips. Biochemical/electrophysiological experiments were performed 24–48 h after transfection.

Electrophysiology

Patch clamp recordings were performed using an EPC9 amplifier and the Pulse software (HEKA, Lambrect, Germany). Microelectrodes (resistance 5–9 MΩ) were prepared with a two-step electrode puller (Narishige, Tokyo, Japan). The standard extracellular/intracellular solution contained (in millimolar) 147 NaCl, 10 HEPES, 13 glucose, 2 KCl, 2 $CaCl_2$ and 1 $MgCl_2$/147 NaCl, 10 HEPES and 10 EGTA, with pH adjusted to 7.3 with NaOH and the osmolarity around 300 mOsm. Other non-standard solutions are detailed when described. Cell membrane potential was held at −60 mV. For current–voltage relationship experiments, voltage ramps (−120 to 70 mV) or voltage steps (−120 to 80 mV with 20 mV increment) were applied in either whole-cell or cell-attached mode. For single-channel recordings, 40 to 60 continuous recordings of 1 s were performed after outside-out configuration was obtained. Drugs were delivered via a rapid solution change system (RSC-200, Bio-logic Science Instruments, Grenoble, France). Acquired data were analysed using Axograph X software (AxoGraph Scientific, Sydney, Australia) and plotted by Kaleidagraph software (Synergy Software, Reading, PA, USA). Data are expressed as mean ± standard error and analysed via Student's *t* test.

Site-directed mutagenesis

Point mutations of mouse Panx1 were introduced using the polymerase chain reaction (PCR) overlap extension method with Accuzyme proof-reading DNA polymerase (Bioline, London, UK). Mutagenised PCR fragments were digested with XbaI (New England Biolabs, Hitchin, UK) and cloned into an expression vector, pcDNA3 (Invitrogen). The full coding sequence of all mutants was confirmed by DNA sequencing.

Plasma membrane protein biotinylation, immunoprecipitation and Western blotting

Transfected HEK cells (35-mm dishes) were washed three times in ice-cold PBS containing 1 mM $CaCl_2$ and 0.5 mM $MgCl_2$ (PBS-CM). Cell surface-expressed proteins were labelled using 1 mg/ml sulfo-NHS-LC-Biotin for 30 min at 4°C in biotinylation buffer (10 mM H_3BO_3, 140 mM NaCl, pH 8.8). Cells were washed with PBS-CM and then incubated 5 min with PBS-CM containing 20 mM Tris pH 8.8. Lysis was performed by scraping cells in 500 μl of lysis buffer (20 mM Hepes, pH 7.4, 100 mM NaCl, 5 mM EDTA, 1% NP40 and the complete set protease inhibitors cocktail (Roche, Welwyn Garden City, UK)). After 30 min of solubilisation at 4°C under agitation, lysates were centrifuged (16,000×*g*, 10 min, 4°C) and the supernatant was collected.

Equal amounts of protein (500–750 μg) were incubated with 20 μl of anti-myc-conjugated agarose beads (Sigma) for 1 h at 4°C on a rotating wheel. Beads were washed three times (5 min at 4°C) in lysis buffer. Proteins were eluted by two incubations with Myc peptide (200 μg/ml; 1 h on a rotating wheel at 4°C). After adding of LDS sample buffer (Invitrogen), proteins were heated at 80°C for 5 min, resolved on Bis–Tris gels (NuPage Novex, Invitrogen) transferred to PVDF membranes and blotted using either streptavidin–HRP or Myc antibody. Signals were revealed using ECL Plus substrate (GE Healtcare, Chalfont St Giles, UK). Blots were analysed by densitometry measurements using the ImageJ software (National Institute of Health, Bethesda, MA, USA).

Immunocytochemistry

Transfected HEK cells were plated on polylysine-coated glass coverslips 24 h prior to immunostaining. After washes with PBS-CM, cells were fixed with 4% paraformaldehyde, 4% sucrose in PBS-CM for 5 min, washed in PBS-CM and then permeabilised by incubation for 5 min in PBS-CM supplemented with 0.1% Triton-X100 and 0.5% BSA. Blocking of non-specific binding sites was performed by incubating cells with PBS-CM containing 0.5% BSA for 30 min. Cells were incubated with the primary antibody for 1 h at 37°C. After PBS-CM/0.5% BSA washes, fluorescent secondary antibodies were added for 1 h at 37°C. After extensive washing, coverslips were mounted. Images were acquired on a Delta Vision RT (Image Solutions, Preston, UK) restoration microscope. The images were collected using a Coolsnap HQ (Photometrics, Maidenhead, UK) camera with a Z optical spacing of 0.2 μm. Raw images were then deconvolved using the Softworx software and maximum intensity projections of these deconvolved images are shown in the results.

For labelling of plasma membrane, living cells were incubated in PBS-CM+2 mM sulfo-NHS-LC-biotin (Pierce) for 30 min at 4°C before quenching (with PBS-CM, 20 mM Tris pH 8.8) and fixation. Streptavidin–Texas Red was used to reveal plasma membrane proteins. Images were analysed by densitometry measurements using NIH ImageJ software.

Results

Membrane localisation of Panx1 in HEK cells

The sub-cellular localisation of Panx1 expressed in HEK cells was visualised by immunocytochemistry using a Myc-tagged construct. After cell-surface biotinylation performed on living cells, membrane proteins and mPanx1-Myc were detected using streptavidin–Texas Red and Myc-FITC antibody, respectively. The maximum intensity of Panx1 staining was at or close to the plasma membrane (Fig. 1a).

The membrane localisation of mPanx1-Myc was further analysed by determining the levels of expression from cell-surface biotinylation (Fig. 1b). After Myc immunoprecipitation, the membrane fraction of Panx1 was detected using streptavidin–HRP. Relative membrane expression of Panx1 measured by streptavidin labelling was about fivefold higher for K36E point substituted mutant as compared to the wildtype (WT) protein (Fig. 1b). This mutation reverses the charge of lysine located at the inner (cytoplasmic) end of the first transmembrane domain. Total protein expression was unaffected, as judged by immunoprecipitation with the Myc antibody (Fig. 1b). These results indicate that while Panx1 is localised in close proximity to the cell surface (Fig. 1a), it is not predominantly incorporated in the plasma membrane (Fig. 1b). In line with this observation, the Panx1 currents, defined by carbenoxolone-sensitive component

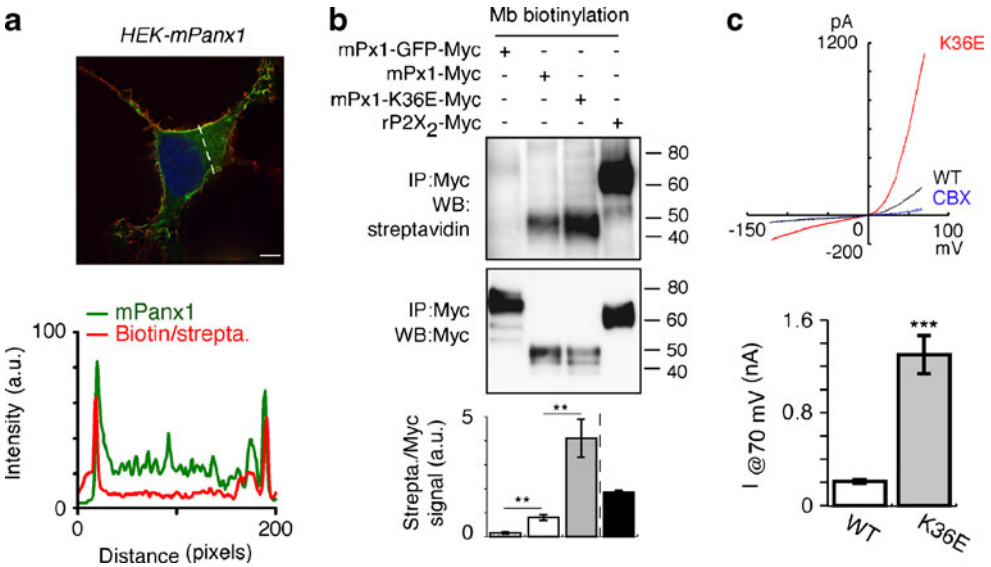

Fig. 1 Membrane localisation of Panx1 expressed in HEK cells. **a** mPanx1-Myc staining revealed an apparent plasma membrane localisation in transfected HEK cells. mPanx1-Myc was stained with a Myc antibody (*green*) and plasma membrane proteins with streptavidin–Texas Red (*red*) after biotinylation on living cells. A densitometry measurement on a section of the cell (indicated by the *dashed line*) demonstrated a high correlation of both signals. **b** However, cell-surface biotinylation followed by immunoprecipitation with Myc-agarose beads showed a low level of plasma membrane expression of the wild-type mPanx1-Myc, compared with that of mPanx1-K36E-Myc. The GFP-fused mPanx1 construct abolished membrane expression. $rP2X_2$-Myc construct was used as a positive control. Plasma membrane protein and total protein were detected by streptavidin–HRP and Myc-HRP, respectively. Ratios between the membrane (indicated by streptavidin signal) and total (Myc signal) proteins were normalised to mPanx1-Myc. **c** A sevenfold increase in the current amplitude (measured at 70 mV) of mPanx1-K36E mutant compared with the wild type. ***$p<0.001$ significance level

measured at 70 mV, were also about seven times larger in K36E point mutation (K36E, 1300.2±164.4 pA (n=17); wild type, 207.3±14.4 pA (n=87); Fig. 1c).

Panx1 forms an anion-permeable channel

Expression of Panx1 in HEK293 cells resulted in the appearance of a large outward current at positive potentials (at 70 mV, 270±19 pA, n=236) that was never observed in non-transfected cells (30±3 pA, n=83; Fig. 2a). This current was reversibly blocked by CBX (10 to 100 μM) and by 5-nitro-2-(3-phenylpropylamino)benzoic acid (NPPB) (100 μM); the CBX/NPPB-sensitive component was defined as the Panx1 current (Fig. 2a). When all the sodium in the extracellular solution was replaced by *N*-methyl-D-glucamine (NMDG), the reversal potential of Panx1-mediated current was unchanged (n=10, Fig. 2b). In control studies, we measured the reversal potential of currents elicited by ATP (100 μM) in cells expressing rat $P2X_2$ receptors: in this case, replacement of extracellular sodium by NMDG shifted the reversal potential of the current from 0 mV to −81±2.6 mV (n=6, Fig. 2b).

Replacement of extracellular chloride with aspartate, glutamate or gluconate produced a significant shift of the Panx1 current reversal potential (by 39.4±2.2 mV (n=5), 33.5±1.3 mV (n=6), or 34.7±1.5 mV (n=6), respectively) (Fig. 2c). In control experiments, these substitutions did not change the reversal potential of the ATP-activated current mediated by $P2X_2$ receptors (n=6). When extracellular chloride was partially substituted by aspartate, the reversal potential showed an intermediate change ($[Cl^-]_o$ 155 mM: −0.2±0.3 mV, n=20; 57 mM: 15.8±0.7 mV, n=6; 8 mM: 39.4±2.2 mV, n=5) (Fig. 3a). Substitution of extracellular Cl^- with mannitol resulted in larger shifts in the reversal potential ($[Cl^-]_o$ 57 mM: 25.0±1.2 mV, n=6; 8 mM: 63.7±3.3 mV, n=5) (Fig. 3a). The slope of the line fitting the relation between the reversal potential and the $\log_{10}$ of the chloride concentration was 30.3 mV/log unit (aspartate substitution) and 48.8 mV/log unit (mannitol substituion) (Fig. 3b); this is consistent with the relative aspartate permeability (0.16, see below). Conversely, when intracellular chloride was reduced (aspartate substitution) from 147 to 50 and 10 mM, the reversal potential shifted from −0.2±0.3 mV (n=20) to −16.7±0.8 mV (n=4) and −39.5±1.0 mV (n=5), respectively.

Relative permeabilities of Panx1 to anions

The relative permeabilities for several monovalent anions were determined by measuring the reversal potential when extracellular chloride was substituted with the relevant anion (except for fluoride, in which case, intracellular chloride was replaced to prevent extracellular calcium chelation) (Fig. 4a, b). The relative permeability ratios were calculated

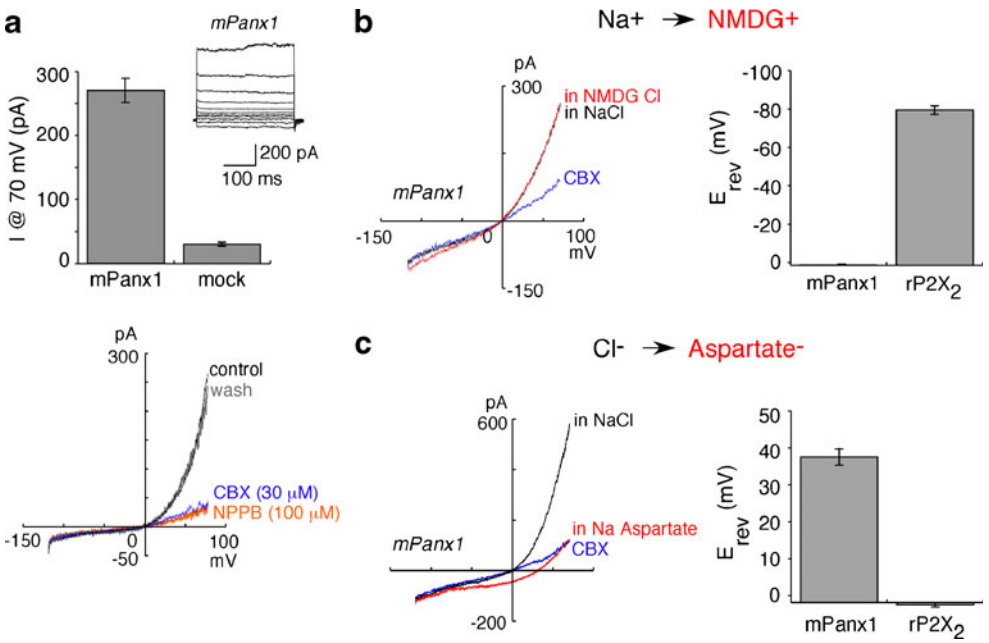

Fig. 2 Panx1 is permeable to chloride but not to sodium. **a** Outwardly rectifying whole-cell currents were recorded from mPanx1- but not mock-transfected HEK cells. The mPanx1 currents were reversibly blocked by CBX (30 μM) or NPPB (100 μM). **b** mPanx1 currents reversed at 0 mV when there was no Na^+ or Cl^- gradient across the cell membrane (*black traces*). Replacement of extracellular Na^+ by $NMDG^+$ (147 mM $NMDG^+$ outside vs. 147 mM^+ Na inside) did not affect mPanx1 currents (*red trace*) but shifted the reversal potential of the $rP2X_2$ currents to −81±2.6 mV. **c** Substitution of extracellular Cl^- by aspartate right-shifted the reversal potential of the mPanx1 currents by 39.4±2.2 mV (*red trace*) without affecting the $rP2X_2$ currents

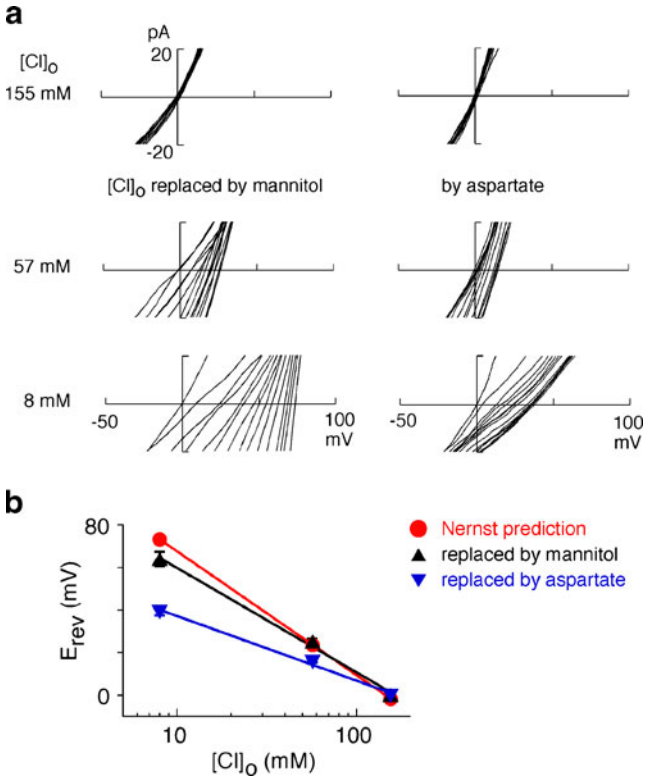

Fig. 3 Shift of Panx1 reversal potential by changing transmembrane gradients for Cl^-. **a** When $[Cl^-]_o$ was reduced from 155 mM to 57 mM or 8 mM ($[Cl^-]_i$ was kept at 147 mM), the mPanx1 reversal potential shifted from −0.2±0.3 mV to 25.0±1.2 mV and 63.7±3.3 mV (mannitol substitution, *left*), or to 15.8±0.7 mV and 39.4±2.2 mV (aspartate substitution, *right*). **b** The reversal potentials and the respective logarithm of chloride concentrations are fitted by a linear relationship with slopes of $E_{rev}/\log([Cl^-]_o)$ and being −58.2 mV/log unit (Nernstian prediction), −48.8 mV/log unit (mannitol substitution) or −30.3 mV/log unit (aspartate substitution)

using the Goldman–Hodgkin–Katz equation. Table 1 summarises the reversal potentials obtained for various anion replacements and their permeability ratios to chloride. The rank order of permeabilities was: $NO_3^->I^->Br^->Cl^-> F^- >>$aspartate$^-\approx$glutamate$^-\approx$gluconate$^-$. The average amplitudes of the Panx1 current (measured at 70 mV) recorded in NO_3^-, I, Cl^- and aspartate$^-$ were 646±99 pA (n=14), 382± 53 pA (n=9), 207±14 pA (n=87) and 68±6.3 pA (n=38) (Fig. 4a, b).

Unitary Panx1 currents

Strong depolarisation of outside-out patches from cell expressing Panx1 resulted in the appearance of discrete unitary outward currents. The unitary currents had an amplitude of 5.4±0.6 pA (n=4) at 80 mV, providing an estimate of unitary conductance of 68 pS. Unitary currents were abolished by NPPB (100 μM) (Fig. 5b). No currents were observed at hyperpolarized potentials. In contrast, patches from cells transfected with connexin-43 showed clear single-channel openings at −80 mV. Their amplitude (17.7± 0.9 pA, n=3) at −80 mV provided an estimate of unitary conductance of 220 pS (Fig. 5a), similar to values reported by others [8, 18].

Discussion

Membrane localization of mPanx1 in mammalian cells

Based on immunocytochemistry and plasma membrane biotinylation, it has been proposed previously that rat Panx1 is highly expressed at the plasma membrane [3]. In our study, immunostaining of Panx1-transfected HEK cells confirmed that the protein is trafficked close to the plasma membrane; however, according to plasma membrane biotinylation, it is poorly expressed within the membrane (see Fig. 1). Incidentally, similar cytosolic localisation was also demonstrated for several types of chloride channels for example for bestrophin-1 [19]. The availability of Panx1 channels through its relocation into the plasmalemma could be controlled by signalling pathways, as was recently demonstrated in Jurkat cells where caspase-3 and caspase-7 activation substantially increased Panx1 currents [6].

Different plasmalemmal appearance of Panx1 may reflect a species difference—we have used mouse Panx1 whereas Boassa et al. [3] used rat. A single amino acid difference might account for differences in membrane insertion, as we observed in the case of K36E mutation (on mPanx1 plasmalemmal presence). This amino acid substitution (K36E) also increased its function measured by membrane currents. This result suggests that this mutation may modify a motif involved in the interaction of Panx1 with others proteins, which regulate either its intracellular retention or plasma membrane stabilisation.

Panx1 forms an anionic channel

Substitution of sodium ions in the extracellular solution with NMDG did not affect Panx1 conductance. In contrast, changes in chloride concentration, either extracellular or intracellular, shifted the reversal potential of Panx1 currents as expected from changes in transmembrane chloride gradients (Figs. 2 and 3). When the extracellular chloride was partially replaced by aspartate, the slope of the relationship between reversal potential and the $\log_{10}$ of the chloride concentration differed from the predicted theoretical value (58 mV-fold per log unit) assuming the channel with exclusive chloride permeability. However when the Cl^- was replaced with mannitol, the slope became much closer to the Nerstian prediction. This difference arises from the fact that the channel is also significantly permeable to the monovalent anion used in these experiments (e.g. aspartate). The rank order of

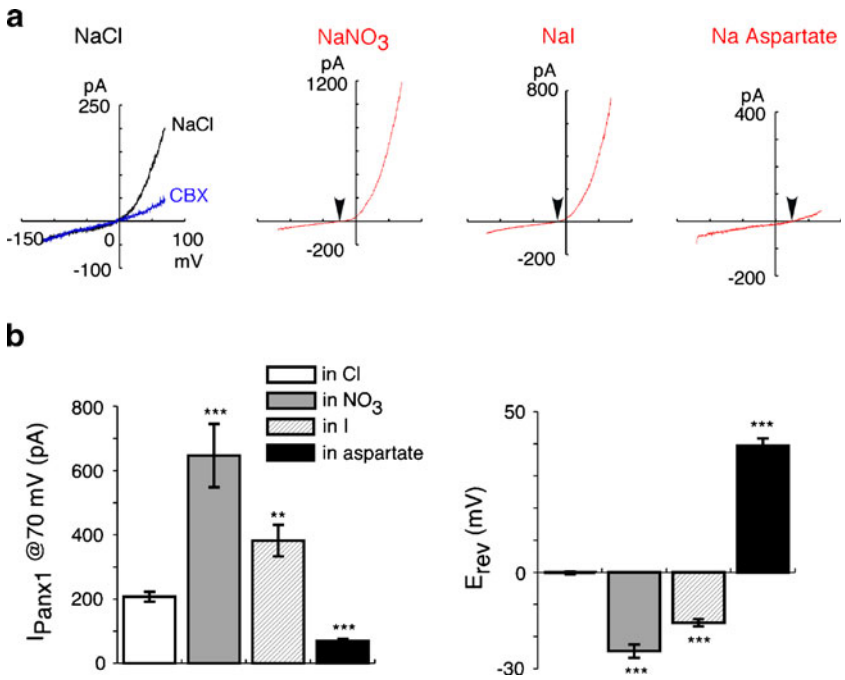

Fig. 4 Permeation of Panx1 channel to other monovalent anions. **a** mPanx1 displayed greater permeation to NO_3^- and I^- than to Cl^- but smaller permeation to aspartate$^-$. *Arrows* indicate the voltages at which the mPanx1 currents reversed. **b** When Cl_o^- was replaced by the relevant anion, the average mPanx1 current amplitudes were 207.3±14.4 pA (in Cl^-), 646.4±99.1 pA (in NO_3^-), 382.2±53.1 pA (in I^-) and 68.5±6.3 pA (in aspartate$^-$). The corresponding reversal potentials were −0.2±0.3 mV (in Cl^-), −24.5±2.5 mV (in NO_3^-), −15.7±1.1 mV (in I^-) and 39.4±2.2 mV (in aspartate$^-$). ***$p<0.001$ significance level, **$p<0.01$ significance level

permeabilities (Table 1) determined using the Goldman–Hodgkin–Katz equation was NO_3^->I^->Br^->Cl^->F^-≫aspartate$^-$≈glutamate$^-$≈gluconate$^-$. This order is the inverse of that of the size of the respective ions, and agrees with the sequence of halide mobility in free solution (the Eisenman selectivity sequence I, [29]). Furthermore, this order of anion permeabilities is characteristic for many other anion channels including the newly identified TMEM16A channel [30]. Consistent with this demonstration of anion permeability was the observation that the Panx1-mediated currents were inhibited by known chloride channel blockers, with order of potency CBX>DIDS≈NPPB≈SITS>IAA-94≈DCPIB>glibenclamide (also see [16]).

Unitary Panx1 currents

Unitary currents were readily activated following membrane depolarisation to levels more positive than +10 mV, but these were never seen in non-transfected cells. These unitary Panx1 currents were inhibited by chloride channel blocker NPPB at the same concentrations that blocked the whole-cell currents. The single-channel conductance of about 68 pS was very different from the single-channel activity recorded for connexin 43, whose unitary currents were activated at negative potentials and had a conductance of ~220 pS.

Table 1 Relative permeation ratios of monovalent anions through mouse Panx1

	E_{rev} (mV)	P_x/P_{Cl}
F^-	−11.2±1.1 [a]	0.69
Cl^-	−0.2±0.3	1.00
Br^-	−8.2±0.9	1.33
I^-	−15.7±1.1	1.81
NO_3^-	−24.5±2.5	2.58
Aspartate$^-$	39.4±2.2	0.16

[a] Cl^- was replaced by other monovalent anions from the extracellular side, except by F^- from the intracellular side

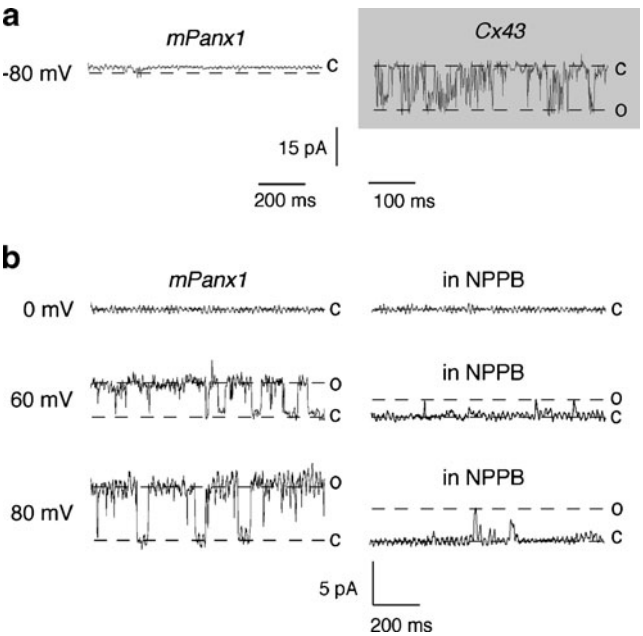

Fig. 5 Conductance of single Panx1 channel. Outside-out patch-clamp recordings of mPanx1 or Cx43 from HEK cells. Patches were held at −60 mV before depolarisation/hyperpolarisation. **a** Comparison of single-channel activity in membrane patches excised from cells expressing mPanx1 or Cx43 channel; at −80 mV Panx1 fails to activate whereas Cx43 channels show high activity. **b** Single-channel openings of mPanx1 at different potentials, and their block by 100 μM NPPB

Panx1 signalling functions may not be associated with hemichannel

From the very beginning of research on pannexins, they were considered to act as gap junctional channels [20]; subsequently when the Panx-associated gap junctions were not identified in variety of tissues, pannexins were assigned the hemichannel role [17]. There is a considerable wealth of data demonstrating the involvement of Panx1 proteins in diverse cellular functions and signalling cascades. Indeed, various manipulations with the levels of Panx1 expression or functional status, have identified their role in release of ATP and cytokines [1, 13, 22, 23], stimulation of inflammatory responses [27], shaping of synaptic responses in hippocampus [28], providing a hemichannel-related conductance in astrocytes [12] and mediating intercellular communication in taste buds [7]. Conceptually, the signalling role of connexin was, almost by default, associated with their hemichannel activity; it was generally considered (although never shown directly) that Panx1 effects are mediated primarily by the opening of large transmembrane pore.

This interpretation, however, is not devoid of certain inconsistencies. First and foremost the Panx1-mediated currents were not recorded in native preparations. Second, the experiments on ectopic expression systems [4, 16, 22] consistently show activation of Panx1 channels only at positive membrane potentials (with a threshold of 10 mV, and appreciable currents at >40 mV). Most of the living cells are unable to generate such strong depolarisations; and even in excitable cells (e.g. neurones) these levels of membrane potential are attained for a very short periods during action potential overshoot. However, this apparent activation threshold is artificially determined by the (semi-equal) chloride gradient provided in the recording solutions. In real cells where such Cl^- equilibrium does not exist, a high $[Cl^-]_o$/low $[Cl^-]_i$ gradient allows Panx1 currents to be activated at a much more negative potential (around −30 to −50 mV depending on the actual $[Cl^-]_i$). Third, direct comparison of Panx1-mediated dye uptake and Panx1-mediated currents showed clear dissociation between these two processes [22], thus questioning the pore-forming ability of pannexin proteins. Our results demonstrate that Panx1 forms an anion channel with relatively low conductance. This anion channel can be permeable to ATP (similarly to other anion channels [9]) thus forming a conduit for ATP release.

Acknowledgements The authors would like to thank Austin Sitko and Rosemary Gaskell for cell culture assistance. This study was supported by the Biotechnology and Biological Sciences Research Council, UK.

References

1. Bao L, Locovei S, Dahl G (2004) Pannexin membrane channels are mechanosensitive conduits for ATP. FEBS Lett 572:65–68
2. Baranova A, Ivanov D, Petrash N, Pestova A, Skoblov M, Kelmanson I, Shagin D, Nazarenko S, Geraymovych E, Litvin O, Tiunova A, Born TL, Usman N, Staroverov D, Lukyanov S, Panchin Y (2004) The mammalian pannexin family is homologous to the invertebrate innexin gap junction proteins. Genomics 83:706–716
3. Boassa D, Ambrosi C, Qiu F, Dahl G, Gaietta G, Sosinsky G (2007) Pannexin1 channels contain a glycosylation site that targets the hexamer to the plasma membrane. J Biol Chem 282:31733–31743
4. Bruzzone R, Hormuzdi SG, Barbe MT, Herb A, Monyer H (2003) Pannexins, a family of gap junction proteins expressed in brain. Proc Natl Acad Sci USA 100:13644–13649
5. Bruzzone R, Barbe MT, Jakob NJ, Monyer H (2005) Pharmacological properties of homomeric and heteromeric pannexin hemichannels expressed in Xenopus oocytes. J Neurochem 92:1033–1043
6. Chekeni FB, Elliott MR, Sandilos JK, Walk SF, Kinchen JM, Lazarowski ER, Armstrong AJ, Penuela S, Laird DW, Salvesen GS, Isakson BE, Bayliss DA, Ravichandran KS (2010) Pannexin 1 channels mediate 'find-me' signal release and membrane permeability during apoptosis. Nature 467:863–867
7. Dando R, Roper SD (2009) Cell-to-cell communication in intact taste buds through ATP signalling from pannexin 1 gap junction hemichannels. J Physiol 587:5899–5906
8. Eghbali B, Kessler JA, Spray DC (1990) Expression of gap junction channels in communication-incompetent cells after stable transfection with cDNA encoding connexin 32. Proc Natl Acad Sci USA 87:1328–1331
9. Fields RD (2011) Nonsynaptic and nonvesicular ATP release from neurons and relevance to neuron-glia signaling. Semin Cell Dev Biol 22:214–219
10. Huang Y, Grinspan JB, Abrams CK, Scherer SS (2007) Pannexin1 is expressed by neurons and glia but does not form functional gap junctions. Glia 55:46–56
11. Huang YJ, Maruyama Y, Dvoryanchikov G, Pereira E, Chaudhari N, Roper SD (2007) The role of pannexin 1 hemichannels in ATP release and cell-cell communication in mouse taste buds. Proc Natl Acad Sci USA 104:6436–6441
12. Iglesias R, Dahl G, Qiu F, Spray DC, Scemes E (2009) Pannexin 1: the molecular substrate of astrocyte "hemichannels". J Neurosci 29:7092–7097
13. Kawamura M Jr, Ruskin DN, Masino SA (2010) Metabolic autocrine regulation of neurons involves cooperation among pannexin hemichannels, adenosine receptors, and KATP channels. J Neurosci 30:3886–3895
14. Locovei S, Bao L, Dahl G (2006) Pannexin 1 in erythrocytes: function without a gap. Proc Natl Acad Sci USA 103:7655–7659
15. Locovei S, Wang J, Dahl G (2006) Activation of pannexin 1 channels by ATP through P2Y receptors and by cytoplasmic calcium. FEBS Lett 580:239–244
16. Ma W, Hui H, Pelegrin P, Surprenant A (2009) Pharmacological characterization of pannexin-1 currents expressed in mammalian cells. J Pharmacol Exp Ther 328:409–418
17. MacVicar BA, Thompson RJ (2010) Non-junction functions of pannexin-1 channels. Trends Neurosci 33:93–102
18. Moreno AP, Eghbali B, Spray DC (1991) Connexin32 gap junction channels in stably transfected cells: unitary conductance. Biophys J 60:1254–1266
19. Neussert R, Muller C, Milenkovic VM, Strauss O (2010) The presence of bestrophin-1 modulates the Ca2+ recruitment from Ca2+ stores in the ER. Pflugers Arch 460:163–175

20. Panchin YV (2005) Evolution of gap junction proteins—the pannexin alternative. J Exp Biol 208:1415–1419
21. Panchin Y, Kelmanson I, Matz M, Lukyanov K, Usman N, Lukyanov S (2000) A ubiquitous family of putative gap junction molecules. Curr Biol 10:R473–474
22. Pelegrin P, Surprenant A (2006) Pannexin-1 mediates large pore formation and interleukin-1β release by the ATP-gated $P2X_7$ receptor. EMBO J 25:5071–5082
23. Pelegrin P, Barroso-Gutierrez C, Surprenant A (2008) $P2X_7$ receptor differentially couples to distinct release pathways for IL-1β in mouse macrophage. J Immunol 180:7147–7157
24. Ransford GA, Fregien N, Qiu F, Dahl G, Conner GE, Salathe M (2009) Pannexin 1 contributes to ATP release in airway epithelia. Am J Respir Cell Mol Biol 41:525–534
25. Reyes JP, Hernandez-Carballo CY, Perez-Flores G, Perez-Cornejo P, Arreola J (2009) Lack of coupling between membrane stretching and pannexin-1 hemichannels. Biochem Biophys Res Commun 380:50–53
26. Schalper KA, Palacios-Prado N, Retamal MA, Shoji KF, Martinez AD, Saez JC (2008) Connexin hemichannel composition determines the FGF-1-induced membrane permeability and free $[Ca^{2+}]_i$ responses. Mol Biol Cell 19:3501–3513
27. Silverman WR, de Rivero Vaccari JP, Locovei S, Qiu F, Carlsson SK, Scemes E, Keane RW, Dahl G (2009) The pannexin 1 channel activates the inflammasome in neurons and astrocytes. J Biol Chem 284:18143–18151
28. Thompson RJ, Jackson MF, Olah ME, Rungta RL, Hines DJ, Beazely MA, MacDonald JF, MacVicar BA (2008) Activation of pannexin-1 hemichannels augments aberrant bursting in the hippocampus. Science 322:1555–1559
29. Wright EM, Diamond JM (1977) Anion selectivity in biological systems. Physiol Rev 57:109–156
30. Yang YD, Cho H, Koo JY, Tak MH, Cho Y, Shim WS, Park SP, Lee J, Lee B, Kim BM, Raouf R, Shin YK, Oh U (2008) TMEM16A confers receptor-activated calcium-dependent chloride conductance. Nature 455:1210–1215